Journal of Applied Research and Technology
ISSN: 1665-6423
jart@aleph.cinstrum.unam.mx
Centro de Ciencias Aplicadas y Desarrollo Tecnológico
México

Kuo, Jian-Long; Cheng, Ming-Te

Optimal Yield Rate in ACF Cutting Process of TFT-LCD Module Using Orthogonal Particle Swarm Optimization Based on Response Surface Design

Journal of Applied Research and Technology, vol. 12, núm. 6, diciembre, 2014, pp. 1165-1175
Centro de Ciencias Aplicadas y Desarrollo Tecnológico
Distrito Federal, México

Optimal Yield Rate in ACF Cutting Process of TFT-LCD Module Using Orthogonal Particle Swarm Optimization Based on Response Surface Design

Jian-Long Kuo*[1] and Ming-Te Cheng[2]

[1,2] Department of Mechanical and Automation Engineering
National Kaohsiung First University of Science and Technology
Nantze, Kaohsiung 811, Taiwan
*JLKUO9999@gmail.com
[1] Department of Mechanical and Automation Engineering
National Kaohsiung First University of Science and Technology
Nantze, Kaohsiung 811, Taiwan.

ABSTRACT
Anisotropic Conductive Film (ACF) is essential material in LCM (Liquid Crystal Module) process. It is used in bonding process to make the driving circuit conductive. Because the price of TFT-LCD is getting lower than before in recent years, the ACF has relatively higher cost ratio. The conventional long bar ACF cutting unit is changed into short bar ACF cutting unit in new bonding technology. However, the new type machine was not optimized in process control and mechanical design. Therefore, the failure rate of new ACF cutting process is much higher than the one of the conventional process. This wastes the ACF material and rework cost is considerably large. How to make the manufacturing cost down effectively and promote the product quality is the main issue to maintain competition capability for the product. Therefore, the orthogonal particle swarm optimization (OPSO) is used to analyze the optimal design problem. The ACF cutting yield rate is selected to be objective function for optimization. The quality characteristic function for yield rate is used in orthogonal particle swarm optimization. Three control factors such as plasma clean speed, ACF peeling speed and ACF cutter spring setting are selected to study the effect of the yield rate. Results show that the proposed method can provide good optimal solution to improve the ACF cutting process for TFTLCD manufacturing process.

Keywords: ACF cutting process, TFT-LCD, response surface method (RSM), plasma clean, orthogonal particle swarm optimization (OPSO).

1. Introduction

The usage amount of ACF material in global TFT-LCD industry is shown as Fig.1. It shows that the annual growth is about 13% in LCD products. The usage amount of ACF material dominates the price of LCD TV modules product. The price of LCD TV has been reduced more than 50% since 2007. Therefore, the cost of the ACF in the TFT-LCD module directly affects the profit space of TFT-LCD products. Conventionally, in long bar ACF cutting process, it is found that the non-conducting area wastes a lot of undesired ACF material. The cutting process in the LCD panel is shown in Fig. 2 [1]-[9].

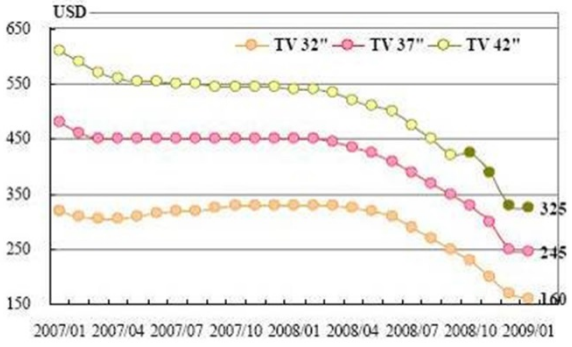

Figure 1. The price of LCD TV over recent years.

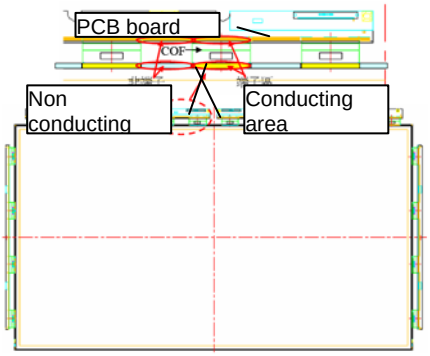

Figure 2. The conventional long bar ACF cutting process in the LCD panel.

The ACF usage percentage in LCD product is shown in Table 1. The ACF usage percentage in LCD products is roughly about 35%. It means that nearly 65% of the ACF usage in cutting process is not required. This increases production cost considerably.

Therefore, in order to save the production cost, the design of conventional long bar ACF cutting unit in Fig. 3 has to be changed into short bar ACF cutting unit in Fig. 4.

panel size	source panel (mm)	gate panel (mm)	source COF (mm)	source COF pcs	gate COF (mm)	gate COF pcs	COF total length(mm)	ACF using rate
19	411.2	252	28.5	10	12.012	3	321.036	48.41%
26	589.6	337.4	41.1	6	27.9	3	330.3	35.63%
31.5	714	408.8	27.9	10	40.4	3	400.2	35.64%
32	717.35	412	27.9	10	40.1	3	399.3	35.36%
37	840.2	957.4	40.1	12	40.1	8	802	44.62%
40	904.4	1029.2	40.1	12	27.9	8	704.4	36.43%
42	952.64	1086.52	40.1	12	40.1	8	802	39.33%
47	1060.96	1212.88	40.1	12	40.1	8	802	35.27%
52	1182.4	1352	40.1	12	27.9	8	704.4	27.79%
56	2533.2	1444.6	31.1	48	40.1	16	2134.4	53.66%

Table 1. The usage of ACF for different size of product.

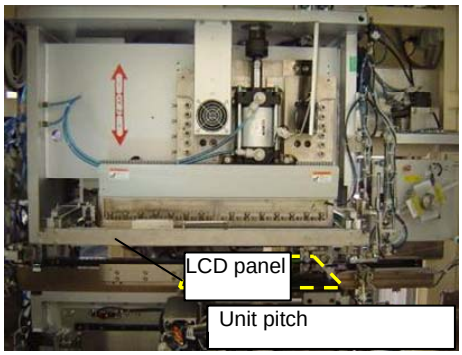

Figure 3. Long bar ACF cutting unit.

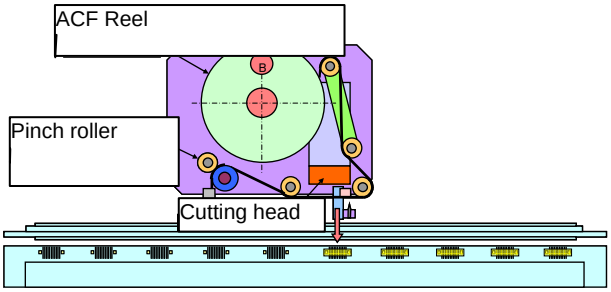

Figure 4. Short bar ACF cutting unit.

Short bar ACF cutting method has the following advantages and disadvantages:

Advantages: 1) Since the ACF material usage is reduced, lower production cost can be achieved. 2) Since the components space placed in the PCB board is increased, more flexible manufacturing methods are provided.

Disadvantages: 1) Cutting more segments increases the tact time under the same manufacturing condition. 2) The failure rate (FR) condition (NG parts/whole cutting segments) of the short bar ACF cutting process is relatively higher than the one of the long bar ACF cutting process.

2. Cutting problem description of ACF cutting process

In TFTLCD manufacturing process, there are many reasons causing failure rate (FR) in the ACF cutting process. Therefore, the peeling phenomena have to be described and defined. The state of peeling phenomena can be divided into upward peeling and downward peeling. The peeling of the location can be defined as cutting from the starting side to the end of peeling. Therefore, by peeling and cutting the ACF material in the ACF cutting process, many unexpected phenomenon possibly occurs.

From the above reasons, it seems that the bad performance of cutter actuator, the bad cutting motion, and the bad peeling condition are the three major reasons to cause the failure rate of ACF cutting process. Therefore, design of experiments (DOE) method based on response surface method (RSM) is used to improve the cleanliness of the panel and change the design condition of the cutter.

3. Problem formulation using response surface method

Response Surface Method（RSM）is generally employed to analyze and describe an unknown and complicated physical problem by design of experiments (DOE) [10]-[13]. In RSM, the mathematical analysis and statistical analysis are jointly utilized to analyze the experimental results to obtain the optimal response solution by discussing the interaction between factors.

When the RSM is employed to analyze the experimental design with a plurality of factors, the experimental runs can be further reduced to achieve the purpose of obtaining optimal solution. Accordingly, the experimental cost can be decreased.

In RSM, two kinds of response surfaces are discussed and defined:

a) Average response surface $E_Z(y(\mathbf{x},\mathbf{z}))$: it represents the average value of a response surface $y(\mathbf{x},\mathbf{z})$ with control factor vector $\mathbf{x}$ and noise factor vector $\mathbf{z}$.

b) Variance response surface $Var_z(y(\mathbf{x},\mathbf{z}))$: it represents the variance of a response surface $y(\mathbf{x},\mathbf{z})$ with control factor vector $\mathbf{x}$ and noise factor vector $\mathbf{z}$.

Some advantages of RSM are described as follows:

a) Not only the average response is evaluated, but also the variance response is evaluated.

b) Both of the average response and variance response are considered to optimize the response surface.

The concept of the RSM is to define the response surfaces of average and variance individually. Therefore, the two response surfaces may be separately analyzed independently. However, the RSM might have trade-off problem between the two response surfaces. The trade-off problem is formulated by using optimization. With the definition of objective function and constraints, the trade-off problem can be solved by using optimization process.

Therefore, the RSM is quite different from the Taguchi method which only uses one index, the SN ratio, to analyze optimal design.

The RSM consists of design steps as follows:

1) Design a combined array in accordance with selected factors and levels

2) Evaluate the average response surface and the variance response surface.

3) Optimize the two response surfaces using OPSO process.

The design flow chart of the RSM is shown in Fig. 5.6.

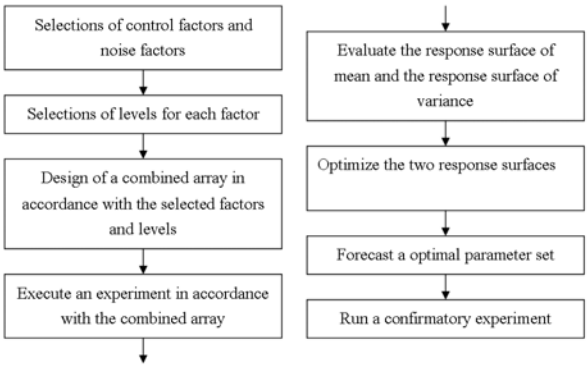

Figure 5. Design flow chart of the RSM.

3.1 Design of combined array

The weakness of Taguchi method is that the average and variance are defined together in a mixed way. A better strategy is to design the combined array with high enough resolution that incorporates both the control factors and noise factors by using response surface method. The average and variance can be discussed separately.

3.2 Definition of two response surfaces

In most of the optimal design case, the relation between the response and independent variables is usually unknown. Therefore, in RSM, the first step is to find a suitable formulation to describe the

adequate relation between the response and the considered independent variables. If the response can be modeled by a regressive model with lower curvature, the response can be modeled by a first-order model.

The average response can be modeled by using regressive analysis. The response function for first-order or second-order regressive model can be formulated by

$$y(\mathbf{x},\mathbf{z}) = b_0 + \mathbf{x}'\mathbf{b} + \mathbf{x}'\mathbf{B}\mathbf{x} + \mathbf{z}'\mathbf{c} + \mathbf{x}'\mathbf{K}\mathbf{z} \quad (1)$$

where

$\mathbf{x}$: vector of controllable factors;

$\mathbf{z}$: vector of uncontrollable factors, or called the noise factors;

b_0 : term of constant;

$\mathbf{b}$: coefficients of the vector of controllable factors;

$\mathbf{B}$: matrix of the interacted term between controllable factors;

$\mathbf{c}$: coefficients of the vector of uncontrollable factors;

$\mathbf{K}$: matrix of the interacted term between controllable factor and uncontrollable factor;

$\mathbf{x}'\mathbf{b}$: linear term of controllable factors;

$\mathbf{x}'\mathbf{B}\mathbf{x}$: interaction term between controllable factors;

$\mathbf{z}'\mathbf{c}$: linear term of uncontrollable factors;

$\mathbf{x}'\mathbf{K}\mathbf{z}$: interaction term between controllable factor and uncontrollable factor;

After finding the response surface $y(\mathbf{x},\mathbf{z})$, the average response surface $E_Z(y(\mathbf{x},\mathbf{z}))$ and variance response surface $Var_z(y(\mathbf{x},\mathbf{z}))$ have to be evaluated by the response surface $y(\mathbf{x},\mathbf{z})$.

The two response surfaces can be modeled by using error propagation theory. If *y* is a function of plural controllable factors including $x_1, x_2 ..., x_n$. That is, the function *y* can be represented as

$$y = f(x_1, x_2 ..., x_n)$$

The average value μ_y, variance σ_y^2, and standard deviation σ_y of the function *y* are further formulated as follows:

$$\mu_y = f\left(\mu_{x_1}, \mu_{x_2}, ..., \mu_{x_n}\right) \quad (2)$$

$$\sigma_y^2 = \left(\frac{\partial f}{\partial x_1}\right)^2 \sigma_{x_1}^2 + \left(\frac{\partial f}{\partial x_2}\right)^2 \sigma_{x_2}^2 + \cdots + \left(\frac{\partial f}{\partial x_n}\right)^2 \sigma_{x_n}^2 \quad (3)$$

$$\sigma_y = \sqrt{\left(\frac{\partial f}{\partial x_1}\right)^2 \sigma_{x_1}^2 + \left(\frac{\partial f}{\partial x_2}\right)^2 \sigma_{x_2}^2 + \cdots + \left(\frac{\partial f}{\partial x_n}\right)^2 \sigma_{x_n}^2} \quad (4)$$

In the following, how to model the two response surfaces by using the error propagation theory is discussed. The following assumptions should be discussed in advance.

a) Assumption 1: $\sigma_x^2 = 0$ for each controllable factor

In design of experiments (DOE) method, three levels for each controllable factor can be selected to evaluate the optimal problem. Therefore, the system variance impacted by each controllable factor should be zero. That is to say, no variance exists among the controllable factors since they are controllable.

b) Assumption 2: $\sigma_z^2 = 1$ and $\mu_z = 0$ for each noise factor

The noise factor is generally an uncontrollable factor, since the noise often unexpectedly occurs in the system. Therefore, the system variance impacted by each noise factor unavoidably exists in the system. To simplify the modeling, both the control factors and noise factors can be transformed into the coded normalized variables for natural variables, ξ.The coded procedure includes the following steps:

1) Estimate the average value $\overline{\xi}$ and the standard deviation σ_ξ of the natural variable.

2) Code and normalize the natural variable by using $\left(\frac{\xi-\overline{\xi}}{\sigma_\xi}\right)$.

After coding, the average value and the standard deviation of the noise factor are $\mu_z = 0$ and $\sigma_z^2 = 1$. That is to say, no average value exists among the noise factors. The standard deviation is normalized to be 1.

The mentioned two assumptions are considered based on error propagation theory to further establish the following two response surfaces.

1) Establish the average response surface

From Eq. (5.38), the average value of Eq. (5.37) can be represented as

$$E_z(y(\mathbf{x},\mathbf{z})) = b_0 + \mathbf{x}'\mathbf{b} + \mathbf{x}'\mathbf{B}\mathbf{x} + \mathbf{z}'\mathbf{c} + \mathbf{x}'\mathbf{K}\mathbf{z} \quad (5)$$

Referring again to assumption 2, the average value of the noise factor is set to zero **z**=0. Therefore, the Eq.（5.41）can be rewritten

$$E_z(y(\mathbf{x},\mathbf{z})) = b_0 + \mathbf{x}'\mathbf{b} + \mathbf{x}'\mathbf{B}\mathbf{x} \quad (6)$$

2) Establish the variance response surface

By using the error propagation theory, the response surface of variance can be represented as

$$Var_z(y(\mathbf{x},\mathbf{z})) = \sum\left(\frac{\delta y}{\delta x_i}\right)^2 \sigma_{xi}^{\ 2} + \sum\left(\frac{\delta y}{\delta z_i}\right)^2 \sigma_{zi}^{\ 2} \quad (7)$$

Referring again to assumption 1, the variance of the control factor is set to zero $\sigma_x^2 = 0$. Therefore, the Eq. (5. 43) can be expressed as:

$$Var_z(y(\mathbf{x},\mathbf{z})) = \sum\left(\frac{\delta y}{\delta x_i}\right)^2 (0)^2 + \sum\left(\frac{\delta y}{\delta z_i}\right)^2 \sigma_{zi}^{\ 2} = \sum\left(\frac{\delta y}{\delta z_i}\right)^2 \sigma_{zi}^{\ 2} \quad (8)$$

4. System formulation of cutting process using response surface method

Dual response surfaces method is used to formulate the optimization problem. Based on response surface method, the average response surface and variance response surface have to be found first. The optimization problem is to maximize the objective function formulated by average response surface subject to constraint condition formulated by the variance response surface. In order to verify the validity of the optimization process and find optimal solution set, testing case is illustrated in the following.

The central point experiment means that the spring gram elastic constant is 50 g. The plasma cleaning velocity is 150 mm/s. The cutter peeling speed is 150 mm/s. The three control factors and two noise factors defined for response surface method are shown in Table 2.

	Spring gram	Plasma speed	Peel speed	Temp	Pressure
	x1	*x2*	*x3*	*Noise 1*	*Noise 2*
Level 1	30g	100mm/s	100mm/s	100℃	0.1Mpa
Level 2	50g	150mm/s	150mm/s	120℃	0.15Mpa
Level 3	70g	200mm/s	200mm/s	140℃	0.2Mpa

Table 2. Level Definition for the three control factors and two noise factors.

The combinational array is listed in Table 3 for the response surface method. The temperature and pressure are selected as noise factors. The experimental runs of the yield rate values for the ACF cutting process for are listed in Table 3. Besides, the four central point repeated experiments are required to be measured in Table 4.

Spring gram(g)	Plasma speed(mm/sec)	Peel speed (mm/sec)	Temp (℃)_	Pressure (Mpa)	Yield (%)
x1	x2	x3	Noise 1	Noise 2	y
-1(30)	-1(100)	-1(100)	-1(100)	1(0.2)	96.93
1(70)	-1(100)	-1(100)	-1(100)	-1(0.1)	98.71
-1(30)	1(200)	-1(100)	-1(100)	-1(0.1)	95.62
1(70)	1(200)	-1(100)	-1(100)	1(0.2)	97.93
-1(30)	-1(100)	1(200)	-1(100)	-1(0.1)	92.90
1(70)	-1(100)	1(200)	-1(100)	-1(0.1)	98.46
-1(30)	1(200)	1(200)	-1(100)	1(0.2)	94.79
1(70)	1(200)	1(200)	-1(100)	-1(0.1)	97.57
-1(30)	-1(100)	-1(100)	1(135)	-1(0.1)	97.31
1(70)	-1(100)	-1(100)	1(135)	1(0.2)	98.74
-1(30)	1(200)	-1(100)	1(135)	1(0.2)	95.73
1(70)	1(200)	-1(100)	1(135)	-1(0.1)	97.56
-1(30)	-1(100)	1(200)	1(135)	1(0.2)	96.80
1(70)	-1(100)	1(200)	1(135)	-1(0.1)	98.52
-1(30)	1(200)	1(200)	1(135)	-1(0.1)	95.02
1(70)	1(200)	1(200)	1(135)	1(0.2)	97.64

Table 3. Combinational Array in Response Surface Method.

Spring gram(g)	Plasma speed(mm/sec)	Peel speed (mm/sec)	Temp (℃)_	Pressure (Mpa)	Yield (%)
x1	x2	x3	Noise 1	Noise 2	y
0(50)	0(150)	0(150)	0(120)	0(0.15)	96.94
0(50)	0(150)	0(150)	0(120)	0(0.15)	96.38
0(50)	0(150)	0(150)	0(120)	0(0.15)	96.38
0(50)	0(150)	0(150)	0(120)	0(0.15)	96.37

Table 4. Combination table and experiment results for the four central point experiments.

For the four repeated experimental values, the average value is calculated as:

$$\overline{y_c} = (96.94+96.38+96.38+96.37)/4=96.51 \quad (9)$$

For the experimental data in combinational array, the average value is also computed as:

$$\overline{y_F} = (96.93+96.71+95.62+97.93+92.90+98.46+94.79+97.57+97.31 +98.74+95.73+97.56+96.8+98.52+95.02+97.64)/16 = 96.89 \quad (10)$$

The sum of variance for the curvature is:

$$SS_C = \frac{n_F n_C (\overline{y}_F - \overline{y}_C)^2}{n_F + n_C} \Rightarrow \frac{(16)(4)(96.51-96.89)^2}{16+4} = 0.46 \quad (11)$$

The sum of variance for the error is:

$$SS_E = \sum_{i=1}^{n_C} (y_i - \overline{y}_C)^2$$
$$= (96.94-96.51)^2 + (96.38-96.51)^2$$
$$+(96.38-96.51)^2 + (96.37-96.51)^2$$
$$= 0.23 \quad (12)$$

The F-statistic value is calculated as:

$$F = \frac{SS_C/1}{SS_E/(n_C-1)} = \frac{0.46/1}{0.23/(4-1)} = 5.903 \quad (13)$$

It shows that the curvature is not large. Therefore, it is suitable to use the first-order regressive model. The derived average response surface is computed as:

$$E_Z(y(\mathbf{x},\mathbf{z})) = b_0 + \mathbf{x}'\mathbf{b} + \mathbf{x}'\mathbf{B}\mathbf{x}$$
$$= 96.81538 + 1.251375x_1 - 0.40775x_2 - 0.40752x_3$$
$$- 0.5905x_1x_2 + 0.334183x_1x_3 + 0.20087x_2x_3 \quad (14)$$

The corresponding 3-D surface plot and contour plot are shown in Fig. 5.

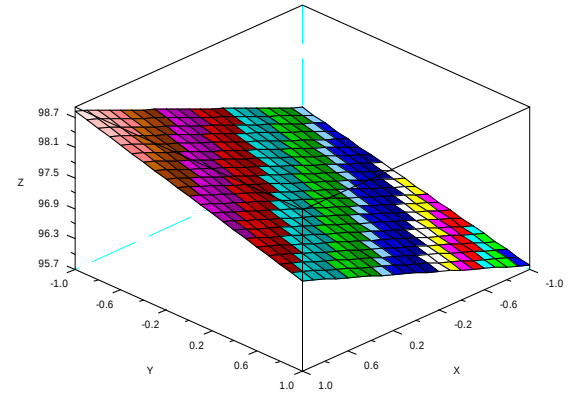

(a) 3-D surface plot of average response surface for first-order regression model.

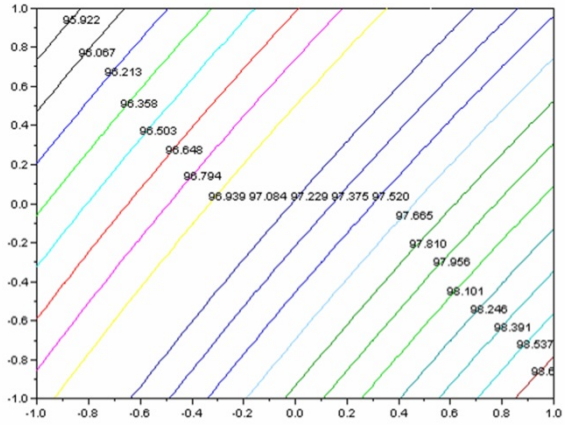

(b) contour plot of the average response for first-order regression model.

Figure 6. Average response surface for the response surface method.

The variance response surface is derived as:

$$Var_Z(y(\mathbf{x},\mathbf{z})) = \sum (\partial y/\partial z_i)^2 \sigma_{zi}^2 = (\partial y/\partial z_1)^2 \sigma_{z1}^2 + (\partial y/\partial z_2)^2 \sigma_{z2}^2 \quad (15)$$

Therefore

$$\partial y/\partial z_1 = 0.275113 - 0.3012x_1 - 0.27197x_2 + 0.256035x_3$$
$$\partial y/\partial z_2 = 0.23827 - 0.18736x_1 - 0.1967x_2 + 0.22009x_3 \quad (16)$$

If the standard deviation for z_1, z_2 is set to $\sigma_{z_1}=1$, $\sigma_{z_2}=1$ respectively,

$$\begin{aligned} Var_z(\,y(\mathbf{x},\mathbf{z})) &= (0.275113\text{-}0.3012x_1\text{-}0.27197x_2+0.256035x_3)^2(1)^2 \\ &\quad +(0.23827\text{-}0.18736x_1\text{-}0.1967x_2+0.22009x_3)^2(1)^2 \\ &= 0.13245957\text{-}0.25501168x_1\text{-}0.243380545x_2\text{-}0.245758413x_3 \\ &\quad +0.237541788x_1x_2-0.23670669x_1x_3-0.22581199x_2x_3 \\ &\quad +0.125823847x_1^2+0.112659057x_2^2+0.113993328x_3^2 \end{aligned} \tag{17}$$

The corresponding 3-D surface plot and contour plot are shown in Fig. 6.

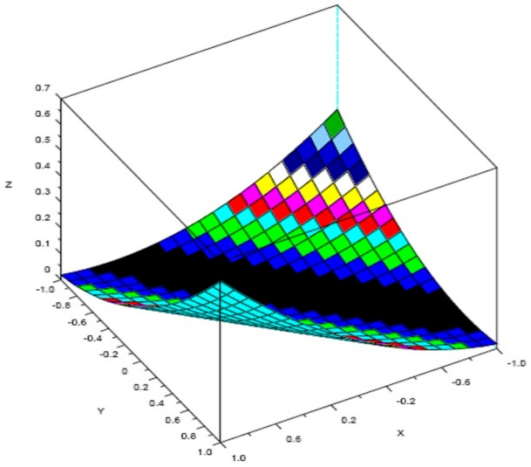

(a) 3-D surface plot of the variance response surface for first-order regression model.

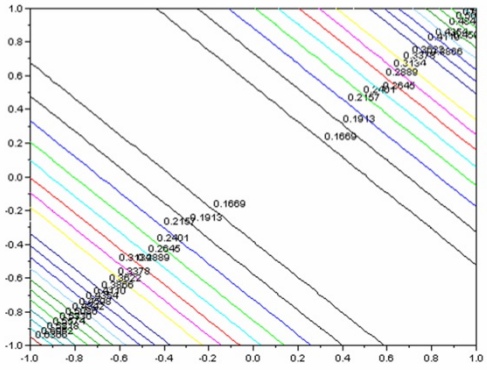

(b) Contour plot of variance response surface for first-order regression model.

Figure 7. Variance response surface for the response surface method.

Therefore, the variance response surface is used to be the constrained condition for the optimization problem.

$$\begin{aligned} Var_z(\,y(\mathbf{x},\mathbf{z})) &= (0.275113\text{-}0.3012x_1\text{-}0.27197x_2+0.256035x_3)^2(1)^2 \\ &\quad +(0.23827\text{-}0.18736x_1\text{-}0.1967x_2+0.22009x_3)^2(1)^2 \\ &= 0.13245957\text{-}0.25501168x_1\text{-}0.243380545x_2\text{-}0.245758413x_3 \\ &\quad +0.237541788x_1x_2-0.23670669x_1x_3-0.22581199x_2x_3 \\ &\quad +0.125823847x_1^2+0.112659057x_2^2+0.113993328x_3^2<100 \end{aligned} \tag{18}$$

where the following inequalities should be satisfied.

$$\begin{aligned} -1.0 \le x_1 \le 1.0 \\ -1.0 \le x_2 \le 1.0 \\ -1.0 \le x_3 \le 1.0 \end{aligned} \tag{19}$$

5. Orthogonal particle swarm optimization process

With the above derived system model by response surface method, the optimization process is performed to derive the optimal solution set for this problem. However, the optimal solution may be located anywhere in the range of -1.0 and +1.0. The local optimal solution may not be the optimal in the global region. Therefore, the OPSO process is used to derive the optimal solution in an efficient way. The local searching and global searching are going simultaneously. Global optimal solution can be found.

By adding the random seeds into formulation, the OPSO can jump out of the local optimal solution if the global solution is more optimal than the local solution. In the following, the OSPO formulation is performed. Since in the response surface method, the nonlinear problem is formulated as first-order model problem. However, the curvature for this model is large. That means the nonlinearity property is still heavy in this problem. This influences the searching process when finding the optimal solution.

The particle swarm optimization originates from the emulation of the group dynamic behavior of animal. For each particle in a group, it is not only affected by its respective particle, but also affected by the overall group. There are position and velocity vectors for each particle. The searching

method combines the experience of the individual particle with the experience of the group. For a particle as a point in a searching space with D-dimensional can be defined as [14]-[19].

The i-th duty cycle particle associated with the MPPT controller can be defined as:

$$X_{id} = \left(x_{i1}, x_{i2}, ..., x_{iD}\right) \tag{20}$$

where d=1,2,…,D and i=1,2,...,PS, PS is the population size. The respective particle electric power and group electric power associated with each duty cycle X_{id} are defined as

$$P_{pd} = \left(p_{p1}, p_{p2}, ..., p_{pD}\right) \tag{21}$$

$$P_{gd} = \left(p_{g1}, p_{g2}, ..., p_{gD}\right) \tag{22}$$

The refreshing speed vector can be defined as

$$V_{id} = \left(v_{i1}, v_{i2}, ..., v_{iD}\right) \tag{23}$$

The refreshing position and velocity vectors can be expressed as

$$V_{id}^{n+1} = V_{id}^{n} + c_1 \times rand() \times \left(P_{pd} - X_{id}^{n}\right) + c_2 \times rand() \times \left(P_{gd} - X_{id}^{n}\right) \tag{24}$$

$$X_{id}^{n+1} = X_{id}^{n} + V_{id}^{n} \tag{25}$$

When the searching begins, the initial solution is set. In the iteration process, the particle is updated by the value coming from group duty cycle and particle duty cycle. The convergence condition is dependent on the minimum of the average square error of the particle. Both the experience of the individual particle and the experience of the group are mixed into the searching process.

In the optimization problem, there might be a local minimum problem. The optimal solution might jump into a local trap and can not jump out of the trap. Actually, a local minimum point does not represent a global solution in a wide range. In the group experience, random function is used to jump out of the local interval. An inertia weighting factor is considered in this algorithm to increase the convergence rate. An inertia weighting factor is added in the following expression. The modified formula can be expressed as:

$$V_{id}^{n+1} = W \times V_{id}^{n} + c_1 \times rand() \times \left(P_{pd} - X_{id}^{n}\right) + c_2 \times rand() \times \left(P_{gd} - X_{id}^{n}\right) \tag{26}$$

$$W = W_{\max} - \frac{W_{\max} - W_{\min}}{gen_{\max}} \times gen \tag{27}$$

where the c_1 and c_2 are both constants. $W_{\max}$ is The initial weighting value. $W_{\min}$ is the final weighting value. *gen* is the number of current generation. $gen_{\max}$ is the number of final generation. However, the above mentioned is actually a kind of linear modification. To make the algorithm suitable for nonlinear searching problem, there is many nonlinear modification methods proposed to refresh the velocity vector. The modified term is defined as the key factor. By setting the learning factors c_1 and c_2 which are larger than 4.0, the modification for the speed vector is expressed as:

$$V_{id}^{n+1} = K \times \begin{bmatrix} V_{id}^{n} + c_1 \times rand() \times \left(P_{pd} - X_{id}^{n}\right) \\ + c_2 \times rand() \times \left(P_{gd} - X_{id}^{n}\right) \end{bmatrix} \tag{28}$$

$$K = \frac{2}{\left|2 - \left(c_1 + c_2 - \sqrt{\left(c_1 + c_2\right)^2 - 4 \times \left(c_1 + c_2\right)}\right)\right|} \tag{29}$$

A modified PSO method called orthogonal PSO (OPSO) is proposed to solve the update problem effectively. A simple orthogonal array in Taguchi method is used in this algorithm to help the update.

6. Orthogonal array algorithm in OPSO method

To run the Taguchi method, two functions are defined first. The particle swarms are composed of individual particle swarm O_{id} and group particle swarm A_{id} .

$$O_{id} = X_{id}^{n} + WV_{id}^{n} + c_1 \times rand() \times \left(P_{pd} - X_{id}^{n} \right) \quad (30)$$

$$A_{id} = X_{id}^{n} + WV_{id}^{n} + c_2 \times rand() \times \left(P_{gd} - X_{id}^{n} \right) \quad (31)$$

These two functions are specified as two control factors in Taguchi method. Two levels are defined for the control factors. Therefore, the orthogonal array has two factors and two levels. The electric power calculating from the MPPT converter is used as the measured value in orthogonal array. Assume that the optimal solution is expressed as Q_{id} . The Q_{id} is adopted to refresh the particle position and velocity vectors as shown in the following expression. The particle refreshing process in OPSO optimization is illustrated in Fig. 7.

$$V_{id}^{n+1} = Q_{id} - X_{id}^{n} \quad (32)$$

$$X_{id}^{n+1} = Q_{id} \quad (33)$$

7. Discussion

This paper has achieved the aim of finding optimal solution for the TFTLCD manufacturing process. The derived optimal solution can provided the manufacturing process under the optimal operating condition.

By using the response surface method with OPSO method, the mathematical model for this problem is provided and verified. This will be very helpful to associated industrial application.

The optimal solution can be found and located at the ends of the range. Global solution is found instead of local solution. Results show that the proposed mathematical method has the capability of finding appropriate searching process.

8. Conclusion

Through the analysis of response surface method combined with OPSO process, the optimal solution is found. The optimal solution is located at (x_1 , x_2 , x_3)=(0.98,-0.97,-0.98). The corresponding optimal solution for yield rate is 99.30. The local optimal solution is avoided and the proposed OPSO algorithm can find the optimal solution at the endpoints globally. In OPSO, global and local optimal ranges are searched at the same time. The related confirmation experiments show that the proposed methodology can provide good prediction with the practical case.

It is convinced that the proposed optimal parameter solution solved by OPSO algorithm can increase the cutting yield rate of ACF cutting process for the TFT-LCD module.

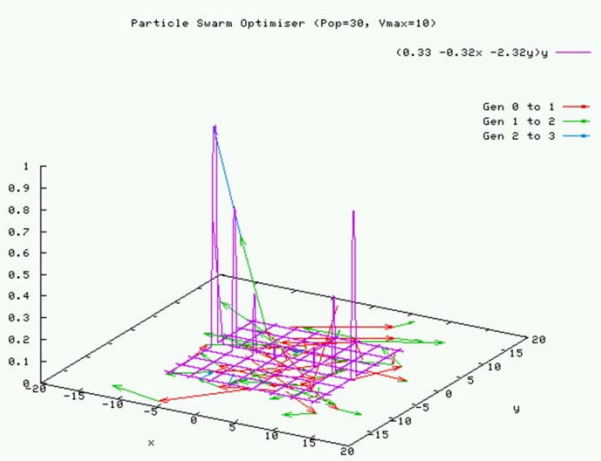

(a) Refreshing process from first generation to third generation.

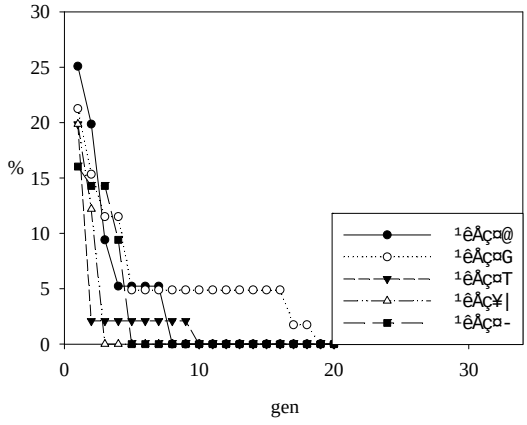

(b) Error percentage from first generation to fifth generation.

Figure 8. Illustration of particle refreshing process and convergence rate in OPSO optimization.

Acknowledgments

The authors would like to thank Chi-Mei Inc. for providing the required testing equipment. The editing help by Tzeng Tseng is also appreciated.

References

[1] Su C.D., Quality project, “Chinese Republic of China Quality Academic society,” 2002.

[2] Li H.H., “Taguchi method-quality design's principle and the practice,” stand high, 2005.

[3] Luo J.X., “Taguchi quality project direction, Chinese production center of pressure,” 1999.

[4] Lee N.C., “Reflow soldering process and troubleshooting: SMT, BGA, CSP and Flip Chip technologies,” 2005.

[5] Yang Z.Y., “Profit with the Taguchi method to improve the LCD manufacturing process, Feng Chia University,” Industrial Engineering and Systems Management Institute Master's thesis, 2006.

[6] Hitachi Chemical, “Interconnection Technologies Using Anisotropic Conductive Adhesive Films For Output And Input Leads,” 2004, Aug. 10.

[7] Hitachi High-Technology, “ACF attch FR improve report,” 2007, Oct. 1.

[8] Kuo C.L., “Using plasma technology for clean process,” Creating nano tech. Co., Ltd., 2004, Apr. 13.

[9] Hsu J.C., “Plasma setting and testing report,” Chi-Mei Opto Co., Ltd., 2000, July 29.

[10] Koyamada K. et al., “Parameter optimization technique using the response surface methodology,” Annual International Conference of the IEEE EMBS, 2004, pp. 2909-2912.

[11] Myers R. H. and Montgomery D. C., “Response surface methodology,” John Wiley & Sons Inc., 1995.

[12] Park J. M. et al., “Rotor design on torque ripple reduction for a synchronous reluctance motor with concentrated winding using response surface methodology,” IEEE Transactions on Magnetics, vol. 42, no. 10, 2006, pp. 3479-3481.

[13] Lee D. J. et al., “Design and optimization of a linear actuator for subminiature optical storage devices,” IEEE Transactions on Magnetics, vol. 41, no. 2, 2005, pp. 1055-1057.

[14] Shi Y. and Eberhart R., “A modified Particle swarm optimization,” Proc. of IEEE International Conference on Evolutionary Computation(ICEC), 1998, May, pp. 69-72.

[15] Eberhart R. C. and Shi Y., "Comparing inertia weights and constriction factors in particle swarm optimization," Proc. Congress on Evolutionary Computation, 2000, pp. 84-88.

[16] Ho S. Y. et al., "OPSO: Orthogonal Particle Swarm Optimization and Its Application to Task Assignment Problems," IEEE Trans. On Systems, Man, and Cybernetics, Part A, Vol. 38, No. 2, March, 2008, pp. 288-298.

[17] Jamali S. et al., "An Energy-efficient Routing Protocol for MANETs: a Particle Swarm Optimization Approach," Journal of Applied Research and Technology, Vol. 11, Dec., 2013, pp. 803-812.

[18] Laguna-Sánchez G. A. et al., "Comparative Study of Parallel Variants for a Particle Swarm Optimization Algorithm Implemented on a Multithreading GPU," Journal of Applied Research and Technology, Vol. 7, Dec., 2009, pp. 292-309.

[19] Rezazadeh H. et al., "Linear programming embedded particle swarm optimization for solving an extended model of dynamic virtual cellular manufacturing systems," Journal of Applied Research and Technology, Vol. 7, April, 2009, pp. 83-108.